Available online at www.sciencedirect.com
ScienceDirect
Ceramics International 36 (2010) 727–731
CERAMICS INTERNATIONAL
www.elsevier.com/locate/ceramint

Dielectric relaxation and enhanced multiferroic properties in $YMn_{0.8}Fe_{0.2}O_3$ ceramics prepared by in situ spark plasma sintering

Yan Ma, Xiang Ming Chen *, Yong Jun Wu, Yi Qi Lin

Laboratory of Dielectric Materials, Department of Materials Science and Engineering, Zhejiang University, Hangzhou 310027, China

Received 10 July 2009; received in revised form 3 September 2009; accepted 4 October 2009
Available online 13 November 2009

Abstract

Dielectric characteristics of $YMn_{0.8}Fe_{0.2}O_3$ ceramics prepared by in situ spark plasma sintering (SPS) were evaluated over broad temperature and frequency ranges. An obvious dielectric relaxation was observed in the low temperature range, and it was a thermally activated process following the Arrhenius law. A regular ferroelectric hysteresis loop was detected at 153 K, and the weak ferromagnetic characteristic was observed at room temperature. These results indicated the enhanced multiferroic properties in the Fe-modified $YMnO_3$ ceramics.

Keywords: C. Dielectric properties; C. Ferroelectric properties; C. Magnetic properties; $YMn_{0.8}Fe_{0.2}O_3$ ceramics

1. Introduction

Hexagonal $YMnO_3$ has attracted much scientific attention as one of the promising multiferroic materials. It belongs to the noncentrosymmetric $P6_3cm$ space group with a high ferroelectric transition temperature ($T_C \sim 900$ K) but a low antiferromagnetic transition temperature ($T_N \sim 70$ K) [1–3]. Recent studies have revealed that there is a coupling between the ferroelectric and antiferromagnetic order in hexagonal $YMnO_3$ [4,5].

Hexagonal $YMnO_3$ consists of MnO_5 trigonal bipyramids where each manganese ion is surrounded by three in-plane and two apical oxygen ion. Ferroelectric phase $YMnO_3$ is characterized by a buckling of the layered MnO_5 polyhedra, accompanied by displacements of the Y ions, which leads to a net electric polarization [6]. Below T_N, Mn^{3+} spins interact antiferromagnetically within the hexagonal layers of the structure, indicating that the magnetism is geometrically frustrated (GF) [3,7]. The lower T_N is a limitation for the multiferroic applications of $YMnO_3$, and it is an important issue to improve room temperature ferromagnetic properties of the present material. Recently, many studies on the *A*- and *B*-site substituted $YMnO_3$ have been reported [8–15]. However, only a few investigations are focused on Fe-doped hexagonal $YMnO_3$ [13–15], and the effect of Fe-substitution for Mn on the multiferroic properties of $YMnO_3$ has rarely been studied. $YFeO_3$ has an orthorhombic distorted perovskite structure with space group *Pnma* [16]. Because $YMnO_3$ and $YFeO_3$ both have the perovskite structure, the hexagonal structure of $YMnO_3$ with the noncentrosymmetric space group of $P6_3cm$ might be maintained by substituting a small amount of Fe for Mn, and subsequently the ferroelectricity should also be expected. On the other hand, $YFeO_3$ has a high Néel temperature ($T_N = 640$ K) [16], so the magnetic transition temperature should be increased by Fe substituting for Mn in $YMnO_3$, and the enhanced ferromagnetic properties are expected in Fe-substituted $YMnO_3$ ceramics.

Spark plasma sintering (SPS) has been used widely as a low temperature and rapid method to prepare ceramics and composites [17–20]. In the present work, an in situ SPS technique combined with annealing is used to prepare multiferroic $YMn_{0.8}Fe_{0.2}O_3$ ceramics. The dielectric properties of $YMn_{0.8}Fe_{0.2}O_3$ ceramics were evaluated over broad temperature and frequency ranges, and the multiferroic properties were well investigated.

2. Experimental

High purity raw oxide powders of Y_2O_3 (99.99%), Mn_2O_3 (98%), and Fe_2O_3 (99%) with stoichiometric ratio were carefully weighted and mixed thoroughly, and then ground

* Corresponding author. Tel.: +86 571 87952112; fax: +86 571 87952112.
E-mail address: xmchen59@zju.edu.cn (X.M. Chen).

0272-8842/$36.00
doi:10.1016/j.ceramint.2009.11.002

in anhydrous alcohol for 3 h to get homogeneous mixture. After the mixture was dried, some of them were put into a graphite die and sintered at 1273 K for 5 min in a vacuum of 6 Pa with an SPS apparatus (SPS-1050, SPS SYNTEX Inc., Kanagawa, Japan). During the period of heating and soaking, a pressure of 30 MPa was applied to the sample. The heating rate was 100 K/min from room temperature to 1173 K, 40 K/min from 1173 to 1253 K, and 20 K/min from 1253 to 1273 K. All the in situ synthesized samples by SPS were polished and then annealed at 1473 K in air for 1 h to ensure homogeneity. Density of $YMn_{0.8}Fe_{0.2}O_3$ ceramics after annealing was measured by the Archimedes method. The crystalline phases of the as-sintered and annealed $YMn_{0.8}Fe_{0.2}O_3$ ceramics were characterized by X-ray diffraction (D/MAX 2550/PC, Rigaku, Tokyo, Japan) using CuKα radiation. The microstructures were evaluated on the polished surfaces of $YMn_{0.8}Fe_{0.2}O_3$ ceramics after annealing with a field emission scanning electron microscopy (S-4800, Hitachi, Tokyo, Japan). The polished surfaces were thermally etched at 1448 K for 1 h before observation. The dielectric, conductive, ferroelectric and magnetic characterizations were conducted for $YMn_{0.8}Fe_{0.2}O_3$ ceramics after annealing. The dielectric characteristics were measured with a broadband dielectric spectrometer (Turnkey Concept 50, Novocontrol Technologies, Germany) in a broader range of temperature (123–573 K) and frequency (10–1,000,000 Hz), where the silver paste was adopted as the electrodes. The polarization–electric field (*P–E*) hysteresis loops were evaluated at 153 K and 10 Hz by Precision Materials Analyzer (RT Premier II, Radiant Technologies, Inc., NM), and the dc resistivity was also measured. The magnetic properties were evaluated by the Quantum Design Polyfunctional Physical Property Measurement System (PPMS-9, Quantum Design, TN).

3. Results and discussions

Fig. 1 shows the sintering behavior of the $YMn_{0.8}Fe_{0.2}O_3$ ceramics in situ synthesized by SPS. When the temperature increases from room temperature to 673 K, a small thermal expansion is observed, and then a relatively large thermal expansion takes place till approximately 993 K. The shrinkage initiates at about 1153 K, and it increases rapidly when the temperature increases up to 1273 K. Subsequently, almost no shrinkage is observed until the soaking period, suggesting that the densification almost completes at temperature below 1273 K. After the sample was sintered at 1273 K for 3 min, it begins to expand. Compared with solid state reaction process used in the previous studies [14], the densification temperature in present process is much lower.

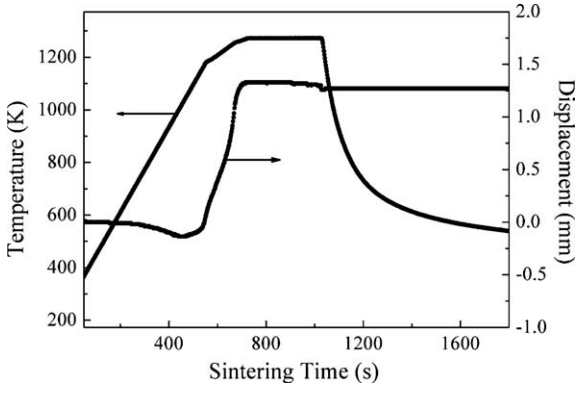

Fig. 1. Shrinkage curve and sample's temperature as a function of sintering time in the process of in situ SPS of $YMn_{0.8}Fe_{0.2}O_3$ ceramics.

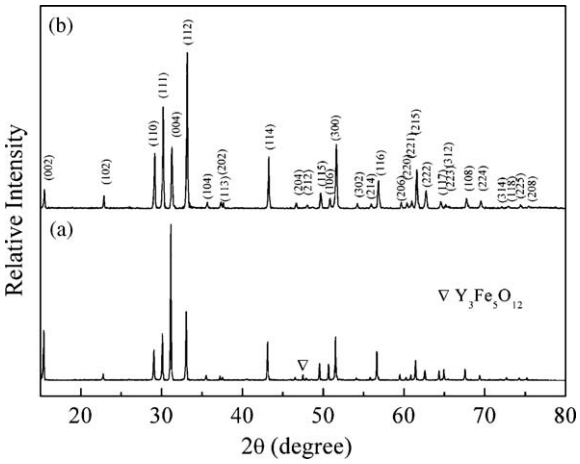

Fig. 2. XRD patterns of $YMn_{0.8}Fe_{0.2}O_3$ ceramics (a) in situ synthesized by SPS at 1273 K for 5 min and (b) subsequently annealed at 1473 K in air for 1 h.

Fig. 2(a) shows the XRD pattern of dense samples in situ synthesized $YMn_{0.8}Fe_{0.2}O_3$ ceramics by SPS at 1273 K for 5 min. The hexagonal phase is synthesized as the major phase, and a small amount of secondary phases ($Y_3Fe_5O_{12}$) is also detected. However, after the subsequent annealing at a high temperature of 1473 K for a short time of 1 h, the $Y_3Fe_5O_{12}$ impurity is removed. As shown in Fig. 2(b), dense $YMn_{0.8}Fe_{0.2}O_3$ ceramics with a single hexagonal phase in space group of $P6_3cm$ is obtained after annealing.

The density of the as-prepared sample is above 95% of the theoretical density according to the results of the Archimedes method. Fig. 3 shows the SEM micrograph on the thermally etched surfaces of $YMn_{0.8}Fe_{0.2}O_3$ ceramics sintered by SPS combined with subsequent annealing, and dense ceramics are

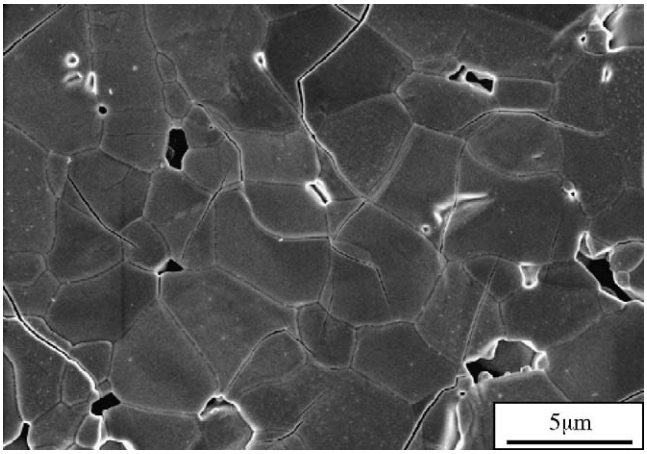

Fig. 3. SEM micrograph on the polished and thermally etched surfaces of $YMn_{0.8}Fe_{0.2}O_3$ ceramics after annealing.

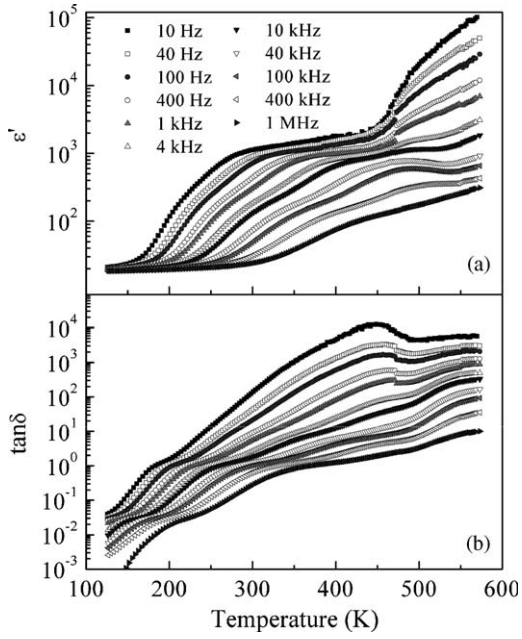

Fig. 4. Temperature dependence of (a) real dielectric permittivity ε' and (b) dielectric loss tan δ of $YMn_{0.8}Fe_{0.2}O_3$ ceramics at different frequencies between 10 Hz and 1 MHz.

well crystallized. Some cracks were observed in the thermally etched surfaces, and this phenomenon is common in $YMnO_3$-based ceramics [21,22].

Fig. 4 shows the temperature dependence of real dielectric permittivity ε' and dielectric loss tan δ of $YMn_{0.8}Fe_{0.2}O_3$ ceramics at different frequencies between 10 Hz and 1 MHz. An obvious dielectric relaxation is observed at the temperature range from 150 to 390 K, and a corresponding inflexion point in the tan δ–T curve is detected, which shifts toward higher temperature with increasing frequency. A dielectric constant step ($\varepsilon' \sim 1000$) is detected on the ε'–T curve in the medium temperature range (300–450 K), and it is weakened at high frequencies. In the higher temperature range, the dielectric constant increases rapidly. Strong frequency dispersion is indicated in the whole testing temperature range.

In order to get a deep insight into the low temperature dielectric relaxation, the frequency dependence of the tan δ inflexion point temperature is studied. As shown in Fig. 5, the variation relation obeys the Arrhenius law,

$$f = f_0 \exp\left(\frac{-E_a}{kT}\right),$$

where f_0 is the preexponential term, E_a the activation energy, and k the Boltzmann's constant. The fitting parameters are obtained as $E_a = 0.38$ eV and $f_0 = 1.30 \times 10^{11}$ Hz. Therefore, the low temperature dielectric relaxation in $YMn_{0.8}Fe_{0.2}O_3$ ceramics is a thermally activated process.

According to the XRD results, $YMn_{0.8}Fe_{0.2}O_3$ ceramics keeps the noncentrosymmetric space group of $P6_3cm$ as pure $YMnO_3$, so the ferroelectric properties should be maintained in $YMn_{0.8}Fe_{0.2}O_3$ at room temperature. Unfortunately, because of

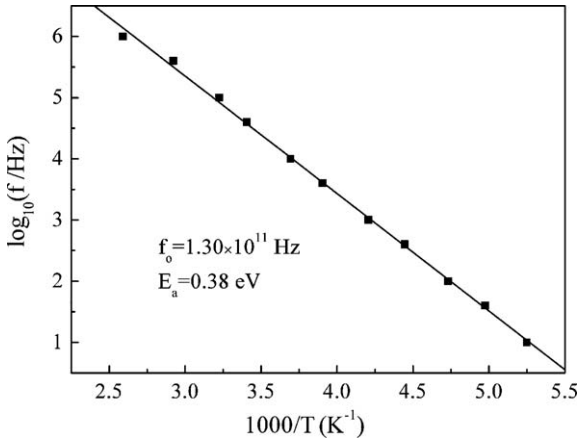

Fig. 5. Frequency dependence of tan δ inflexion point temperature for low temperature dielectric relaxation in $YMn_{0.8}Fe_{0.2}O_3$ ceramics. Symbols are experimental points and solid line is Arrhenius fitting.

the low resistivity (in the order of 10^6 Ω cm) of $YMn_{0.8}Fe_{0.2}O_3$ ceramics, the room temperature P–E loop was measured as a circle (not shown), indicating the samples have serious electrical leakage. Taking into account that the resistivity can be increased with decreasing temperature, we measured the low temperature P–E hysteresis loops of $YMn_{0.8}Fe_{0.2}O_3$

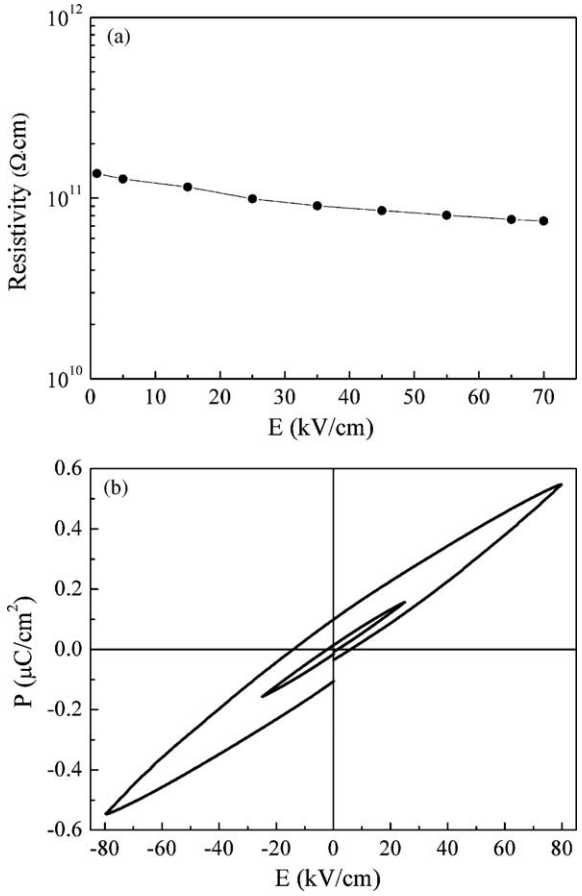

Fig. 6. (a) Electric field dependence of resistivity of $YMn_{0.8}Fe_{0.2}O_3$ ceramics at 153 K. (b) P–E hysteresis loops of $YMn_{0.8}Fe_{0.2}O_3$ ceramics at 153 K under different applied electric field.

ceramics. Fig. 6(a) shows the resistivity of $YMn_{0.8}Fe_{0.2}O_3$ ceramics at 153 K, and it has been greatly increased to the order of 10^{10} to 10^{11} Ω cm. Fig. 6(b) shows the *P–E* hysteresis loops of $YMn_{0.8}Fe_{0.2}O_3$ ceramics at 153 K under different applied electric field, and regular *P–E* hysteresis loops were detected. Although the applied electric field has achieved 80 kV/cm, the *P–E* hysteresis loop is still not saturated, so the saturation electrical field should be higher. When the applied electric field is 80 kV/cm, the spontaneous polarization (P_r) and the coercive field (E_c) of $YMn_{0.8}Fe_{0.2}O_3$ ceramics are 0.10 μC/cm and 14.08 kV/cm^2, respectively. Because the resistivity at 153 K is large enough, and the leakage current is very low, so the *P–E* hysteresis loop should be related to the true ferroelectricity other than the characteristic of lossy dielectric. In addition, because $YMn_{0.8}Fe_{0.2}O_3$ ceramics belong to the noncentrosymmetric space group $P6_3cm$ which is the same as ferroelectric $YMnO_3$, the intrinsic ferroelectricity should be expected.

Fig. 7(a) shows the temperature dependence of ZFC and FC magnetic susceptibility for $YMn_{0.8}Fe_{0.2}O_3$ ceramics under a magnetic field of 0.1 T. The divergence of the ZFC and FC susceptibility is observed till 300 K, so the magnetic transition temperature of $YMn_{0.8}Fe_{0.2}O_3$ should be higher than room temperature. In addition, ZFC magnetic susceptibility reaches a maximum value at 79 K. This temperature is very close to the T_N of pure $YMnO_3$, so the magnetic abnormity should be related to a spin reorientation of Mn ions, revealing a transition to another magnetic phase. Fig. 7(b) shows the *M–H* hysteresis loops of $YMn_{0.8}Fe_{0.2}O_3$ ceramics at different temperatures. Obvious magnetic hysteresis loops are observed even at room temperature, indicating the weak ferromagnetic property of $YMn_{0.8}Fe_{0.2}O_3$ ceramics. The remnant magnetization (M_r) and

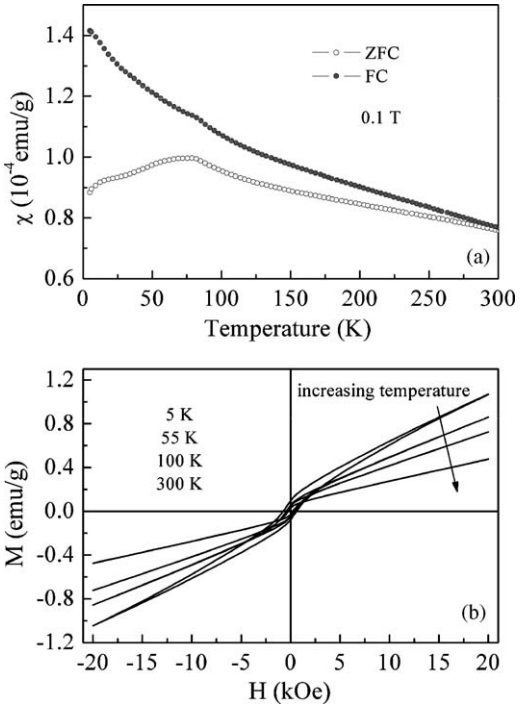

Fig. 7. (a) Temperature dependence of ZFC and FC magnetic susceptibility of $YMn_{0.8}Fe_{0.2}O_3$ ceramics in a field of 0.1 T. (b) *M–H* hysteresis loops of $YMn_{0.8}Fe_{0.2}O_3$ ceramics at different temperatures.

coercive field (H_c) decreases with increasing temperature. Compared with pure $YMnO_3$ which is antiferromagnetic ordered only below 70 K, the magnetic properties of the present $YMn_{0.8}Fe_{0.2}O_3$ ceramics has been greatly improved. This should be attributed to the complex magnetic interaction between the Mn and Fe irons. The co-existence of ferroelectricity and room temperature ferromagnetism in $YMn_{0.8}Fe_{0.2}O_3$ is very interesting, and this might provide a new promising multiferroic material.

4. Conclusions

An obvious dielectric relaxation is observed in the low temperature range in $YMn_{0.8}Fe_{0.2}O_3$ ceramics, which is a thermally activated process. A dielectric constant step is detected in the higher temperature range, and it is weakened at high frequencies. Regular ferroelectric hysteresis loops are detected at 153 K, and a weak ferromagnetic characteristic is observed till room temperature. Through Fe substituting for Mn, the enhanced room temperature ferromagnetic properties are achieved in $YMnO_3$ ceramics together with maintained ferroelectric properties. The present results suggest a new promising multiferroic material.

Acknowledgements

The present work was supported by Natural Science Foundation of China under grant numbers 50832005 and 50672083, and National Basic Research Program under grant no. 2009CB623302.

References

[1] J. Dho, M.G. Blamire, Competing functionality in multiferroic $YMnO_3$, Appl. Phys. Lett. 87 (2005) 252504.
[2] L.J. Wang, S.M. Feng, J.L. Zhu, R.C. Yu, C.Q. Jin, W. Yu, X.H. Wang, L.T. Li, Ferroelectricity of multiferroic hexagonal $TmMnO_3$ ceramics synthesized under high pressure, Appl. Phys. Lett. 91 (2007) 172502.
[3] P.A. Sharma, J.S. Ahn, N. Hur, S. Park, S.B. Kim, S. Lee, J.-G. Park, S. Guha, S.-W. Cheong, Thermal conductivity of geometrically frustrated, ferroelectric $YMnO_3$: extraordinary spin–phonon interactions, Phys. Rev. Lett. 93 (2004) 177202.
[4] Z.J. Huang, Y. Cao, Y.Y. Sun, Y.Y. Xue, C.W. Chu, Coupling between the ferroelectric and antiferromagnetic orders in $YMnO_3$, Phys. Rev. B 56 (1997) 2623–2626.
[5] M. Fiebig, Th. Lottermoser, D. Frohlich, A.V. Goltsev, R.V. Pisarev, Observation of coupled magnetic and electric domains, Nature 419 (2002) 818–820.
[6] B.B. Van Aken, T.T.M. Palstra, A. Filippetti, N.A. Spaldin, The origin of ferroelectricity in magnetoelectric $YMnO_3$, Nat. Mater. 3 (2004) 164–170.
[7] W.R. Chen, F.C. Zhang, J. Miao, B. Xu, X.L. Dong, L.X. Cao, X.G. Qiu, B.R. Zhao, P.C. Dai, Re-entrant spin glass behavior in Mn-rich $YMnO_3$, Appl. Phys. Lett. 87 (2005) 042508.
[8] T. Choi, J. Lee, Bi modification for low-temperature processing of $YMnO_3$ thin films, Appl. Phys. Lett. 84 (2004) 5043–5045.
[9] N. Fujimura, H. Sakata, D. Ito, T. Yoshimura, T. Yokota, T. Ito, Ferromagnetic and ferroelectric behaviors of A-site substituted $YMnO_3$-based epitaxial thin films, J. Appl. Phys. 93 (2003) 6990–6992.
[10] M.C. Sekhar, S. Lee, G. Choi, C. Lee, J.-G. Park, Doping effects of hexagonal manganites $Er_{1-x}Y_xMnO_3$ with triangular spin structure, Phys. Rev. B 72 (2005) 014402.

[11] A.A. Nugroho, N. Bellido, U. Adem, G. Nenert, Ch. Simon, M.O. Tjia, M. Mostovoy, T.T.M. Palstra, Enhancing the magnetoelectric coupling in $YMnO_3$ by Ga doping, Phys. Rev. B 75 (2007) 174435.
[12] T. Asaka, K. Nemoto, K. Kimoto, T. Arima, Y. Matsui, Crystallographic superstructure of Ti-doped hexagonal $YMnO_3$, Phys. Rev. B 71 (2005) 014114.
[13] X.Q. Cao, C.-S. Kim, H.-I. Yoo, Effect of substitution of manganese for iron on the structure and electrical properties of yttrium ferrite, J. Am. Ceram. Soc. 84 (2001) 1265–1272.
[14] A. Veres, J.G. Noudem, S. Fourrez, G. Bailleul, The influence of iron substitution to manganese on the physical properties of $YMnO_3$, Solid State Sci. 8 (2006) 137–141.
[15] S.L. Samal, W. Green, S.E. Lofland, K.V. Ramanujachary, D. Das, A.K. Ganguli, Study on the solid solution of $YMn_{1-x}Fe_xO_3$: structural, magnetic and dielectric properties, J. Solid State Chem. 181 (2008) 61–66.
[16] M. Eibschutz, S. Shtrikman, D. Treves, Mossbauer studies of Fe^{57} in orthoferrites, Phys. Rev. 156 (1967) 562–577.
[17] X.T. Wang, N.P. Padture, H. Tanaka, Contact-damage-resistant ceramic/single-wall carbon nanotubes and ceramics/graphite composites, Nat. Mater. 3 (2004) 539–544.
[18] T. Isobe, K. Daimon, T. Sato, T. Matsubara, Y. Hikichi, T. Ota, Spark plasma sintering technique for reaction sintering of Al_2O_3/Ni nanocomposite and its mechanical properties, Ceram. Int. 34 (2008) 213–217.
[19] Y.F. Zhang, J.X. Zhang, Q.M. Lu, Synthesis of highly textured $Ca_3Co_4O_9$ ceramics by spark plasma sintering, Ceram. Int. 33 (2007) 1305–1308.
[20] Y. Shimojo, R. Wang, Y.J. Shan, H. Izui, M. Taya, Dielectric characters of $0.7Pb(Mg_{1/3}Nb_{2/3})O_3$–$0.3PbTiO_3$ ceramics fabricated at ultra-low temperature by the spark-plasma-sintering method, Ceram. Int. 34 (2008) 1449–1452.
[21] C. Moure, J.F. Fernandez, M. Villegas, P. Duran, Non-ohmic behaviour and switching phenomena in $YMnO_3$-based ceramic materials, J. Eur. Ceram. Soc. 19 (1999) 131–137.
[22] G. Lescano, F.M. Figueiredo, F.M.B. Marques, J. Schmidt, Synthesis and electrical conductivity of $Y_{1-x}Mn_{1-y}O_{3-\delta}$, J. Eur. Ceram. Soc. 21 (2001) 2037–2040.